Characterization of a New Hexasodium Diphosphopentamolybdate Hydrate, $Na_6[P_2Mo_5O_{23}]\cdot 7H_2O$, by ^{23}Na MQMAS NMR Spectroscopy and X-ray Powder Diffraction

Jørgen Skibsted,*,† Michael Brorson,‡ Jørgen Villadsen,‡ and Hans J. Jakobsen†

Instrument Centre for Solid-State NMR Spectroscopy, Department of Chemistry, University of Aarhus, DK-8000 Aarhus C, Denmark, and Haldor Topsøe Research Laboratories, Nymøllevej 55, DK-2800 Lyngby, Denmark

Received March 21, 2000

A novel hexasodium disphosphopentamolybdate hydrate, $Na_6[P_2Mo_5O_{23}]\cdot 7H_2O$, has been identified using X-ray powder diffraction, ^1H, ^{23}Na, and ^{31}P magic-angle spinning (MAS) NMR, and ^{23}Na multiple-quantum (MQ) MAS NMR. Powder XRD reveals that the hydrate belongs to the triclinic spacegroup $P\bar{1}$ with cell dimensions $a = 10.090(3)$ Å, $b = 15.448(5)$ Å, $c = 8.460(4)$ Å, $\alpha = 101.45(6)°$, $\beta = 104.09(2)°$, $\gamma = 90.71(5)°$, and $Z = 2$. The number of water molecules of crystallization has been determined on the basis of a quantitative evaluation of the ^1H MAS NMR spectrum, the crystallographic unit cell volume, and a hydrogen content analysis. The ^{23}Na MQMAS NMR spectra of $Na_6[P_2Mo_5O_{23}]\cdot 7H_2O$, obtained at three different magnetic fields, clearly resolve resonances from six different sodium sites and allow a determination of the second-order quadrupolar effect parameters and isotropic chemical shifts for the individual resonances. These data are used to determine the quadrupole coupling parameters (C_Q and η_Q) from simulations of the complex line shapes of the central transitions, observed in ^{23}Na MAS NMR spectra at the three magnetic fields. This analysis illustrates the advantages of combining MQMAS and MAS NMR at moderate and high magnetic fields for a precise determination of quadrupole coupling parameters and isotropic chemical shifts for multiple sodium sites in inorganic systems. ^{31}P MAS NMR demonstrates the presence of two distinct P sites in the asymmetric unit of $Na_6[P_2Mo_5O_{23}]\cdot 7H_2O$ while the ^{31}P chemical shielding anisotropy parameters, determined for this hydrate and for $Na_6[P_2Mo_5O_{23}]\cdot 13H_2O$, show that these two hydrates can easily be distinguished using ^{31}P MAS NMR.

Introduction

Heteropolyoxyanions of molybdenum have attracted a significant research interest due to the relationships of these species with metal oxide based catalysts and the actual use of some of these polyanions as catalysts.[1,2] The phosphomolybdates constitute a particularly well-researched group of heteropolyoxometalates.[1,3] For example, compounds with Mo:P ratios ranging from 2.5 to 12 have been characterized in the solid state[1] and/or shown to be present in aqueous solution.[4,5] For the diphosphopentamolybdate anion,[4] $[P_2Mo_5O_{23}]^{6-}$, crystal structures have been reported for two sodium salts, $Na_6[P_2Mo_5O_{23}]\cdot 13H_2O$[6] and $Na_6[P_2Mo_5O_{23}]\cdot 14H_2O$,[7] a 4-aminopyridinium salt,[8] and an ethylenediammonium salt.[8] Protonation of the phosphomolybdate anion is possible as seen in, for example, $Na_4[H_2P_2Mo_5O_{23}]\cdot 10H_2O$[7] and $(NH_4)_8Ni(HPO_4)_2(PO_4)_2Mo_{10}O_{30}\cdot 12H_2O$.[9] The $[P_2Mo_5O_{23}]^{6-}$ anion contains five MoO_6 octahedra, which form a pentagonal ring by sharing edges and corners, and two PO_4 tetrahedra connected to each side of the ring and sharing three oxygen atoms with different MoO_6 units. The main difference between the two sodium salt hydrates[6,7] is the interconnection of the $[P_2Mo_5O_{23}]^{6-}$ anions by sodium ions and water molecules, forming the three-dimensional framework.

Phosphorus is a common additive in the heterogeneous, alumina-supported cobalt-molybdenum and nickel-molybdenum hydrotreating catalysts that are used at oil refineries for desulfurization, denitrogenation, and hydrogenation of oil fractions.[10] Although these catalysts in their active (sulfided) state contain MoS_2-like structures, phosphomolybdates are present in some impregnation solutions[11] used for catalyst preparation, and the interaction between phosphomolybdates and alumina is accordingly of importance in determining the activities of the catalysts.[12,13]

Prompted by current research on alumina-supported MoP (model) catalysts, we initiated an investigation of the model compound $Na_6[P_2Mo_5O_{23}]\cdot 13H_2O$ by ^{23}Na and ^{31}P MAS NMR. It was observed that with time this compound transformed into a new hydrate of lower symmetry and with less water of crystallization. In this work we characterize this new hydrate

* Author to whom correspondence should be addressed. Phone: (+45) 8942 3900. Fax: (+45) 8619 6199. E-mail: jskib@kemi.aau.dk.
† University of Aarhus.
‡ Haldor Topsøe Research Laboratories.

(1) Pope, M. T. *Heteropoly and Isopoly Oxometalates*; Spinger-Verlag: Berlin, 1983.
(2) Day, V. W.; Klemperer, W. G. *Science* **1985**, *228*, 4699.
(3) Pope, M. T.; Müller, A. *Angew. Chem., Int. Ed. Engl.* **1991**, *30*, 34.
(4) Pettersson, L. *Acta Chem. Scand.* **1971**, *25*, 1959.
(5) Pettersson, L.; Andersson, I.; Öhman, L.-O. *Inorg. Chem.* **1986**, *25*, 4726.
(6) Strandberg, R. *Acta Chem. Scand.* **1973**, *27*, 1004.
(7) Hedman, B. *Acta Crystallogr., Sect. B* **1977**, *33*, 3083.
(8) Aranzabe, A.; Wéry, A. S. J.; Martin, S.; Gutiérrez-Zorrilla, J. M.; Luque, A.; Martinez-Ripoll, M.; Román, P. *Inorg. Chim. Acta* **1997**, *255*, 35.
(9) Andersen, E. K.; Villadsen, J. *Acta Chem. Scand.* **1993**, *47*, 748.
(10) Topsøe, H.; Clausen, B. S.; Massoth, F. E. In *Catalysis-Science and Technology*; Anderson, J. R., Boudart, M. Eds.; Springer: Berlin, 1996; Vol. 11, pp 1−302.
(11) van Veen, J. A. R.; Sudmeijer, O.; Cornelis, A. E.; de Wit, H. *J. Chem. Soc., Dalton Trans.* **1986**, 1825.
(12) van Veen, J. A. R.; Hendriks, P. A. J. M.; Andréa, R. R.; Romers, E. J. G. M.; Wilson, A. E. *J. Phys. Chem.* **1990**, *94*, 5282.
(13) Kraus, H.; Prins, R. *J. Catal.* **1996**, *164*, 251.

10.1021/ic000309j CCC: $19.00
Published on Web 08/18/2000

using a combination of X-ray powder diffraction and solid-state ^1H, ^{23}Na, ^{31}P magic-angle spinning (MAS) and ^{23}Na multiple-quantum (MQ) MAS NMR spectroscopy. The latter technique[14,15] improves spectral resolution, since the ^{23}Na MAS NMR spectra of the central transition exhibit complex line shapes, because of overlap of several second-order quadrupolar patterns. The ^{23}Na MQMAS NMR spectra, recorded at three different magnetic fields (7.1, 9.4, and 14.1 T), nicely resolve the individual resonances from the different ^{23}Na sites for the new hydrate. To our knowledge this sample represents the most complex structure studied so far by ^{23}Na MQMAS NMR. Thus, this work mainly focuses on the analysis of the ^{23}Na MQMAS NMR spectra and on the determination of the quadrupole coupling constant (C_Q), the asymmetry parameter (η_Q), and the isotropic chemical shift (δ_{iso}) for each of the sodium sites.

The determination of C_Q and η_Q for ^{23}Na in inorganic compounds is of general interest, since these data reflect the electric field gradients surrounding the sodium atoms while the δ_{iso} values are related to the local electronic structure. Thus, there is an ongoing interest in improving the understanding of the relationships between these parameters and the geometry and site symmetry of the sodium environments.[16−19] For several crystalline materials with only a small number of different sodium sites, these parameters can be determined from ^{23}Na MAS NMR spectra with high precision from either the central transition[20] or the satellite transitions.[21,22] However, for complex systems, techniques such as double-rotation (DOR) NMR,[23,24] dynamic-angle spinning (DAS) NMR,[25,26] or MQMAS NMR[14,15] may advantageously be employed to improve spectral resolution by elimination of the second-order quadrupolar broadening. Of these techniques most studies have recently focused on the MQMAS method, and in particular ^{23}Na MQMAS NMR has been used to further exploit or extend the original experiment (see for example the references cited in refs 27−29). Furthermore, ^{23}Na MQMAS NMR has been routinely employed in studies of sodium-containing inorganic materials[30,31] including sodium cations in zeolites,[32] microporous silicates,[33] and layered silicates.[34] MQMAS NMR spectra of higher complexity have been reported for ^{27}Al in aluminosilicates[35] and in the microporous aluminum phosphate $AlPO_4$-40.[36]

Experimental Section

Synthesis. $Na_6[P_2Mo_5O_{23}]\cdot 13H_2O$. Strandberg's procedure[6] was employed to reproducibly give a powder-XRD-pure orthorhombic, crystalline material. Crystals grew as the mother liquor was allowed to slowly evaporate at room temperature.

$Na_6[P_2Mo_5O_{23}]\cdot 7H_2O$. A sample of $Na_6[P_2Mo_5O_{23}]\cdot 13H_2O$ prepared as described above was at one point split into two batches that were stored in (not necessarily perfectly) sealed containers at room temperature in different laboratories. After one year, powder XRD of one batch of the 13-hydrate showed partial and the other complete conversion into a hitherto unknown pure hydrate. On the basis of ^1H MAS NMR, unit cell volume, and elemental analysis the new hydrate was formulated as a 7-hydrate, i.e., $Na_6[P_2Mo_5O_{23}]\cdot 7H_2O$. Anal. Calcd for $Na_6[P_2Mo_5O_{23}]\cdot 7H_2O$: H, 1.20. Found: H, 1.20. Thermogravimetric analyses (TGA) gave inconclusive results. Attempts to determine the number of waters of crystallization by Karl Fischer titration failed because the compound was insoluble in methanol and/or the water of crystallization did not extract into solution.

X-ray Powder Diffraction. X-ray powder diagrams were recorded on a Philips vertical goniometer equipped with a θ-compensating divergence slit and a diffracted-beam graphite monochromator utilizing Cu Kα radiation. Si powder was used as an external standard. The program TREOR[37] was used for indexing the powder patterns of the pure hydrates followed by least-squares refinement.

NMR Measurements. The solid-state ^{23}Na MAS NMR spectra were obtained at 79.3, 105.8, and 158.7 MHz (i.e., 7.1, 9.4, and 14.1 T) on Varian INOVA-300, -400, and -600 spectrometers, respectively, using home-built CP/MAS NMR probes for 4 and 5 mm o.d. rotors. Rf field strengths of $\gamma B_1/2\pi = 70$, 80, and 75 kHz were employed for the spectra recorded at 7.1, 9.4, and 14.1 T, respectively. Pulse widths of 0.5 μs were used for the single-pulse experiments along with relaxation delays of 1 s. The MQMAS spectra were recorded using the basic two-pulse sequence,[15,38,39] a 36-step phase cycle,[40] and pulse widths for the MQ excitation and conversion pulses corresponding to a 360° pulse (liquid). Each spectrum employed a t_1 increment of 50 μs, 128 t_1 increments, and a relaxation delay of 2 s. Pure absorption-mode, two-dimensional line shapes were obtained by the hypercomplex method.[41] ^{23}Na isotropic chemical shifts are reported relative to an aqueous 1.0 M solution of NaCl. The isotropic triple-quantum shifts (δ_{3Q}) and the F_1 dimension of the ^{23}Na MQMAS spectra are referenced to an aqueous 1.0 M solution of NaCl using ^{23}Na MQMAS spectra of solid NaCl[40] ($\delta_{iso} = 7.17$ ppm and $\delta_{3Q} = 15.24$ ppm) as a second external reference. Simulations and iterative fitting of the experimental spectra were performed using software described elsewhere.[22] The ^{31}P MAS NMR spectra were recorded at 121.42 MHz (7.1 T) using a 7-mm CP/MAS probe, a 45° excitation pulse, and high-power ^1H decoupling. The ^1H MAS NMR spectra were recorded at 399.84 MHz (9.4 T) using a 4-mm CP/MAS probe, a 45° excitation pulse, and a 300-s relaxation delay, corresponding to full spin-lattice relaxation for $Na_6[P_2Mo_5O_{23}]\cdot 7H_2O$ and the external intensity reference samples Na_2HPO_4 and $CH_3COONa\cdot 3H_2O$. ^1H and ^{31}P isotropic chemical shifts are reported relative to neat tetramethylsilane (TMS) and 85% H_3PO_4, respectively.

(14) Frydman, L.; Harwood, J. S. *J. Am. Chem. Soc.* **1995**, *117*, 5367.
(15) Medek, A.; Harwood, J. S.; Frydman, L. *J. Am. Chem. Soc.* **1995**, *117*, 12779.
(16) George, A. M.; Stebbins, J. F. *Am. Mineral.* **1995**, *80*, 878.
(17) George, A. M.; Sen, S.; Stebbins, J. F. *Solid State Nucl. Magn. Reson.* **1997**, *10*, 9.
(18) Koller, H.; Engelhardt, G.; Kentgens, A. P. M.; Sauer, J. *J. Phys. Chem.* **1994**, *98*, 1544.
(19) Fyfe, C. A.; Meyer zu Altenschildesche, H.; Skibsted, J. *Inorg. Chem.* **1999**, *38*, 84.
(20) Samoson, A.; Kundla, E.; Lippmaa, E. *J. Magn. Reson.* **1982**, *49*, 350.
(21) Jakobsen, H. J.; Skibsted, J.; Bildsøe, H.; Nielsen, N. C. *J. Magn. Reson.* **1989**, *85*, 173.
(22) Skibsted, J.; Nielsen, N. C.; Bildsøe, H.; Jakobsen, H. J. *J. Magn. Reson.* **1991**, *95*, 88.
(23) Samoson, A.; Lippmaa, E.; Pines, A. *Mol. Phys.* **1988**, *65*, 1013.
(24) Wu, Y.; Sun, B. Q.; Pines, A.; Samoson, A.; Lippmaa, E. *J. Magn. Reson.* **1990**, *89*, 297.
(25) Mueller, K. T.; Sun, B. Q.; Chingas, C. G.; Zwanziger, J. W.; Terao, T.; Pines, A. *J. Magn. Reson.* **1990**, *86*, 470.
(26) Mueller, K. T.; Wooten, E. W.; Pines, A. *J. Magn. Reson.* **1991**, *92*, 620.
(27) Ding, S.; McDowell, C. A. *J. Magn. Reson.* **1998**, *135*, 61; *Chem. Phys. Lett.* **1999**, *307*, 215.
(28) Kentgens, A. P. M.; Verhagen, R. *Chem. Phys. Lett.* **1999**, *300*, 435.
(29) Madhu, P. K.; GoldBourt, A.; Frydman, L.; Vega, S. *Chem. Phys. Lett.* **1999**, *307*, 41.
(30) Hanna, J. V.; Smith, M. E.; Whitfield, H. J. *J. Am. Chem. Soc.* **1996**, *118*, 5772.
(31) Massiot, D.; Conanec, R.; Feldman, W.; Marchand, R.; Laurant, Y. *Inorg. Chem.* **1996**, *35*, 4957.
(32) Hunger, M.; Sarv, P.; Samoson, A. *Solid State Nucl. Magn. Reson.* **1997**, *9*, 115.
(33) Rocha, J.; Ferreira, P.; Lin, Z.; Brandão, P.; Ferreira, A.; Pedrosa de Jesus, J. D. *J. Phys. Chem. B* **1998**, *102*, 4739.
(34) Hanaya, M.; Harris, R. K. *J. Mater. Chem.* **1998**, *8*, 1073.
(35) Baltisberger, J. H.; Xu, Z.; Stebbins, J. F.; Wang, S. H.; Pines, A. *J. Am. Chem. Soc.* **1996**, *118*, 7209.
(36) Rocha, J.; Lourenco, J. P.; Ribeiro, M. F.; Fernandez, C.; Amoureux, J.-P. *Zeolites* **1997**, *19*, 156.
(37) Werner, P.-E.; Eriksson, L.; Westdahl, M. *J. Appl. Crystallogr.* **1985**, *18*, 367.
(38) Massiot, D.; Touzo, B.; Trumeau, D.; Coutures, J. P.; Virlet, J.; Florian, P.; Grandinetti, P. J. *Solid State Nucl. Magn. Reson.* **1996**, *6*, 73.
(39) Wu, G.; Rovnyak, D.; Sun, B.; Griffin, R. G. *Chem. Phys. Lett.* **1996**, *249*, 210.
(40) Hanaya, M.; Harris, R. K. *J. Phys. Chem. A* **1997**, *101*, 6903.
(41) States, D. J.; Haberkorn, R. A.; Ruben, D. J. *J. Magn. Reson.* **1982**, *48*, 286.

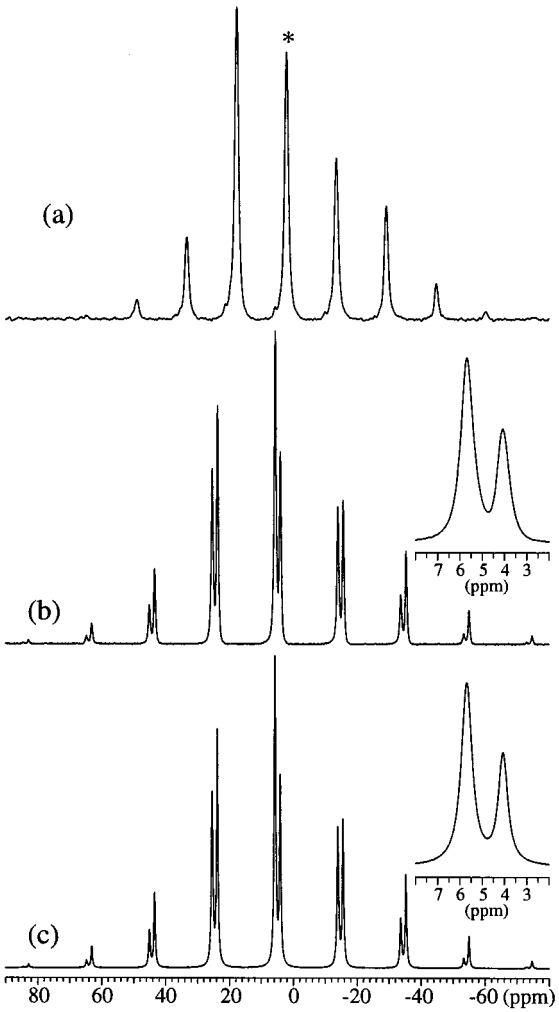

Figure 1. ^{31}P MAS NMR spectra (7.1 T) of (a) $Na_6[P_2Mo_5O_{23}]\cdot 13H_2O$ and (b) $Na_6[P_2Mo_5O_{23}]\cdot 7H_2O$ recorded using high-power ^{1}H decoupling and spinning speeds of $\nu_r = 1.9$ kHz and $\nu_r = 2.4$ kHz, respectively. (c) Simulation of spectrum b) using the δ_σ, η_σ, and δ_{iso} parameters for $Na_6[P_2Mo_5O_{23}]\cdot 7H_2O$ in Table 1 and a 1:1 intensity ratio for the two manifolds of ^{31}P spinning sidebands. The asterisk in part a indicates the isotropic resonance while expansions of these resonances are shown as the right-hand insets in parts b and c.

Results and Discussion

Hexasodium disphosphopentamolybdate tridecahydrate ($Na_6[P_2Mo_5O_{23}]\cdot 13H_2O$) can be formed by slow evaporation of an aqueous solution of H^+, MoO_4^{2-}, and HPO_4^{2-} ions in a $NaClO_4$ medium[4] and unambiguously identified by X-ray powder diffraction using the structural data obtained by single-crystal X-ray diffraction.[6] The structure and purity can also be investigated by ^{31}P MAS NMR as illustrated by the experimental spectrum of a freshly prepared sample of $Na_6[P_2Mo_5O_{23}]\cdot 13H_2O$ shown in Figure 1a. This spectrum reveals a manifold of spinning sidebands which characterizes the chemical shielding anisotropy (CSA) for a single ^{31}P site. This is in agreement with the crystal structure which includes a single ^{31}P site in the asymmetric unit.[6] The ^{31}P CSA parameters (δ_σ and η_σ), obtained by least-squares optimization of simulated to experimental spinning sideband intensities,[22] are listed in Table 1. It is noted that experimental spectra for a range of spinning speeds show no effects from homonuclear ^{31}P−^{31}P dipolar couplings, in agreement with the fact that the PO_4 tetrahedra in $Na_6[P_2Mo_5O_{23}]\cdot 13H_2O$ are situated on each side of the ring of five MoO_6 octahedra with a P−P distance of 3.822 Å.[6]

Following the synthesis and initial ^{31}P MAS NMR analysis, the sample of $Na_6[P_2Mo_5O_{23}]\cdot 13H_2O$ was kept for approximately 1 year at room temperature in a sealed container and then subjected to a new ^{31}P MAS NMR investigation. The corresponding experimental spectrum is shown in Figure 1b and exhibits partially overlapping spinning sideband manifolds from two different ^{31}P sites. Least-squares optimization to the experimental spinning sideband intensities gives the ^{31}P chemical shielding data for the two sites summarized in Table 1. These data are used for the simulated spectrum in Figure 1c which shows that the two ^{31}P sites are present in a 1:1 ratio. Thus, the ^{31}P MAS NMR observations reveal that $Na_6[P_2Mo_5O_{23}]\cdot 13H_2O$ has undergone transformation into a new pure compound, probably a hydrate, which contains two different ^{31}P sites in the asymmetric unit. The ^{31}P chemical shift data in Table 1 shows that the new hydrate can easily be distinguished from $Na_6[P_2Mo_5O_{23}]\cdot 13H_2O$ using ^{31}P MAS NMR. For both $Na_6[P_2Mo_5O_{23}]\cdot 13H_2O$ and the new hydrate the δ_{iso} and δ_σ values are very similar to those reported for orthophosphates.[42,43] This indicates that the PO_4 tetrahedra only share oxygen atoms with the MoO_6 octahedra and that the environments of the PO_4 tetrahedra in the basic $[P_2Mo_5O_{23}]^{6-}$ units are very similar for the two studied samples.

The observation by ^{31}P MAS NMR of a new hydrate is confirmed by the powder XRD pattern shown in Figure 2 where all reflections can be indexed to a single phase belonging to the triclinic space group $P\bar{1}$. A refinement of the reflections gives the cell dimensions $a = 10.090(3)$ Å, $b = 15.448(5)$ Å, $c = 8.460(4)$ Å, $\alpha = 101.45(6)°$, $\beta = 104.09(2)°$, $\gamma = 90.71(5)°$ and a volume of 1251 Å^3 with $Z = 2$. For compounds forming several hydrates the volume of the unit cell per formula unit is often found to be roughly proportional to the number of crystal water molecules (x). Hence, from the data for the 14-hydrate[7] and 13-hydrate[6] one calculates $x = 7.4$ for the new hydrate. A conservative estimate, based on powder-XRD alone, would accordingly be $x = 6-8$. The water content of the hydrate is further investigated by a high-speed ($\nu_r = 15$ kHz) ^{1}H MAS NMR spectrum (not shown), which exhibits a broad and asymmetric isotropic resonance at 3.9 ppm (line width of 4.5 ppm) and its associated spinning sidebands (up to fourth order). This resonance is ascribed to ^{1}H for the H_2O molecules of the hydrate. Employing similar ^{1}H MAS NMR spectra of weighed samples of Na_2HPO_4 and $CH_3COONa\cdot 3H_2O$ as quantitative intensity reference samples allows determination of $x = 7$ (± 0.2) H_2O molecules for the molecular formula of composition $Na_6[P_2Mo_5O_{23}]\cdot xH_2O$ using either of the reference samples. Because hydrogen microanalysis too gives $x = 7$, we therefore formulate the new hydrate as $Na_6[P_2Mo_5O_{23}]\cdot 7H_2O$.

^{23}Na MAS NMR spectroscopy is a very useful tool for determination of the numbers of nonequivalent ^{23}Na sites and their relative occupancies. However, the presence of several distinct sodium sites often complicates the ^{23}Na MAS NMR spectra, because of the second-order quadrupolar broadening of the resonances from the ^{23}Na central transition. This is indeed the case for $Na_6[P_2Mo_5O_{23}]\cdot 7H_2O$, and it may prevent a reliable determination of the number of different sodium sites and of the corresponding δ_{iso} and quadrupole coupling (C_Q and η_Q) parameters. Thus, $Na_6[P_2Mo_5O_{23}]\cdot 7H_2O$ represents a challenge for unravelling these parameters for the individual sodium sites from ^{23}Na MAS and MQMAS NMR experiments.

(42) Turner, G. L.; Smith, K. A.; Kirkpatrick, R. J.; Oldfield, E. *J. Magn. Reson.* **1986**, *70*, 408.
(43) Hartmann, P.; Vogel, J.; Schnabel, B. *J. Magn. Reson., Ser. A.* **1994**, *111*, 110.

Table 1. ^{31}P Chemical Shift Data (δ_σ, η_σ, δ_{iso}, δ_{11}, δ_{22}, and δ_{33})[a] for $Na_6[P_2Mo_5O_{23}]\cdot 13H_2O$ and $Na_6[P_2Mo_5O_{23}]\cdot 7H_2O$

	δ_σ (ppm)	η_σ	δ_{iso}[b] (ppm)	δ_{11} (ppm)	δ_{22} (ppm)	δ_{33} (ppm)
$Na_6[P_2Mo_5O_{23}]\cdot 13H_2O$	46.2 ± 0.8	0.54 ± 0.03	2.2 ± 0.2	37.8 ± 0.9	12.8 ± 0.7	−44.0 ± 0.8
$Na_6[P_2Mo_5O_{23}]\cdot 7H_2O$						
P(1)	43.3 ± 0.8	0.79 ± 0.05	5.6 ± 0.1	44.4 ± 1.3	10.1 ± 1.3	−37.6 ± 0.8
P(2)	61.0 ± 1.0	0.68 ± 0.03	4.1 ± 0.1	55.3 ± 1.2	13.9 ± 0.9	−56.9 ± 1.0

[a] δ_σ and η_σ are defined by the principal elements (δ_{ii}) of the chemical shift tensor as $\delta_\sigma = \delta_{iso} - \delta_{33}$ and $\eta_\sigma = (\delta_{11} - \delta_{22})/\delta_\sigma$ where $\delta_{iso} = {}^1/_3(\delta_{33} + \delta_{22} + \delta_{11})$ and $|\delta_{33} - \delta_{iso}| \geq |\delta_{11} - \delta_{iso}| \geq |\delta_{22} - \delta_{iso}|$. [b] Isotropic chemical shifts relative to 85% H_3PO_4.

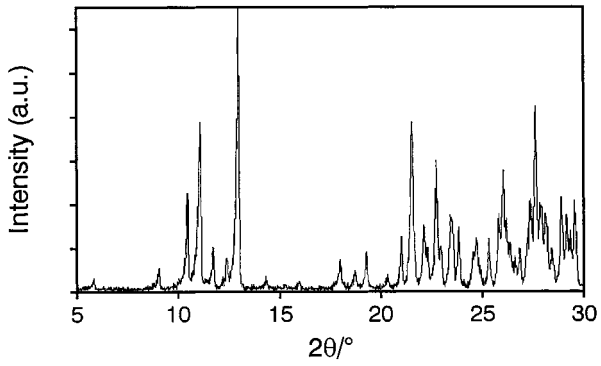

Figure 2. Powder X-ray diffraction diagram of $Na_6[P_2Mo_5O_{23}]\cdot 7H_2O$. The first 48 lines ($2\theta < 31°$) can be indexed in the triclinic system with spacegroup $P\bar{1}$ (No. 2) and the lattice parameters $a = 10.090(3)$ Å, $b = 15.448(5)$ Å, $c = 8.460(4)$ Å, $\alpha = 101.45(6)°$, $\beta = 104.09(2)°$, $\gamma = 90.71(5)°$, $V = 1251$ Å^3, $Z = 2$.

Contour plots of ^{23}Na MQMAS NMR spectra, obtained at 7.1 and 14.1 T, are illustrated in Figure 3 along with projections onto the isotropic (F_1) and anisotropic (F_2) dimensions of the 2D spectra. At both magnetic fields the anisotropic projections resemble the single-pulse ^{23}Na MAS NMR spectra (vide infra), which exhibit a number of singularities, shoulders, and edges arising from second-order quadrupolar line shapes from several distinct ^{23}Na sites. The complexity of the ^{23}Na MAS spectra prevent a straightforward analysis of the overall line shapes for the central transitions without any knowledge of the quadrupolar couplings and isotropic chemical shifts. In contrast, the ^{23}Na MQMAS spectra clearly reveal the presence of six different resonances when the contours in the isotropic and anisotropic dimensions are evaluated. This is best appreciated from the 14.1 T spectrum which exhibits an improved resolution of the six resonances as compared to the MQMAS spectrum at 7.1 T. The projections onto the F_1 dimension exhibit only five distinct resonances for both spectra as the result of a partial overlap of two resonances in this dimension. However, the resonances which overlap in the F_1 dimension are clearly distinguished when the contours in the F_2 dimension are considered.

Summations over the F_1 dimension in ^{23}Na MQMAS NMR spectra recorded at 7.1, 9.4, and 14.1 T are illustrated in Figure 4. The variation in isotropic shifts in the triple-quantum (3Q) dimension (δ_{3Q}) reflects the fact that this parameter depends on δ_{iso} and the quadrupolar product parameter ($P_Q = C_Q(1 + \eta_Q^2/3)^{1/2}$), which exhibit different magnetic field dependencies.[14,15,38] However, it is possible to link together the individual resonances in the F_1 projections at the different magnetic fields using the widths and frequencies of the resonances in the F_2 dimension of the ^{23}Na MQMAS spectra. This results in the assignment (Na(a)−Na(f)) of the resonances illustrated in Figure 4 for the three isotropic spectra. The corresponding isotropic 3Q shifts (δ_{3Q}^{exp}) are determined from an evaluation of the resonance frequencies in the full 2D MQMAS spectra (i.e., for overlapping resonances in the F_1 dimension) and are summarized in Table 2.

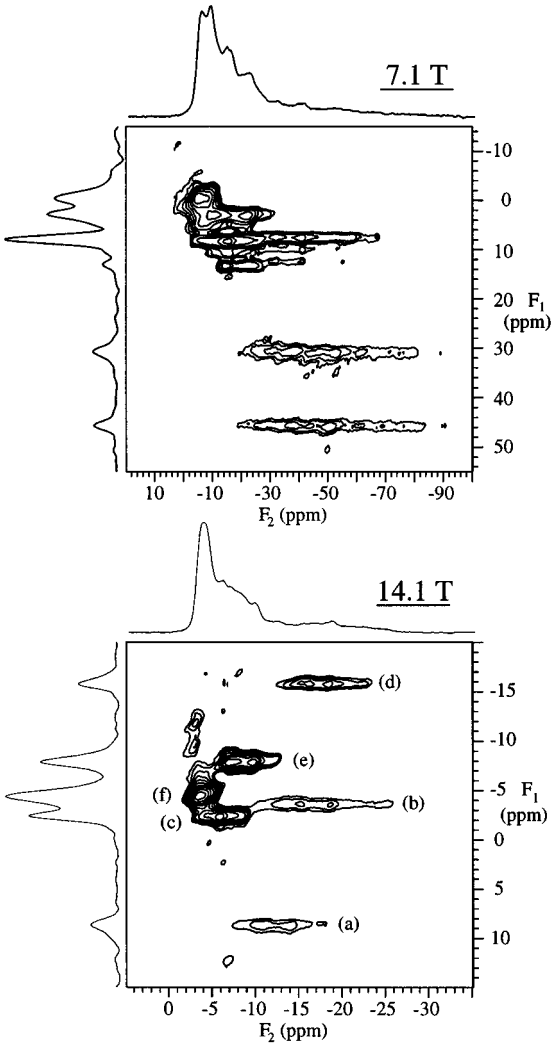

Figure 3. Contour plots of ^{23}Na MQMAS NMR spectra of $Na_6[P_2Mo_5O_{23}]\cdot 7H_2O$ recorded at 7.1 and 14.1 T using spinning speeds of 13.0 and 12.2 kHz, respectively. The projections onto the isotropic (F_1) and anisotropic (F_2) dimensions correspond to summations over the 2D spectra. The assignment of the six resonances is shown for the spectrum recorded at 14.1 T and is given by a−f (see Table 2 and Figure 4).

The observation of isotropic 3Q shifts at different magnetic field strengths allows a determination of δ_{iso} and the quadrupolar effect parameter (P_Q) as shown earlier from ^{27}Al MQMAS experiments at two magnetic fields for the aluminosilicates, leucite and anorthite.[35] This approach employs the relationship

$$\delta_{3Q}^{calc} = \frac{17}{8}\delta_{iso} + \frac{1}{32}\frac{C_Q^2(1+\eta_Q^2/3)}{\nu_L^2}10^6 \qquad (1)$$

which holds for the $p = 0 \rightarrow -3 \rightarrow -1$ coherence transfer pathway, observed in a MQMAS experiment for an $I = {}^3/_2$ nucleus.[14,15,38] The graph in Figure 5 illustrates a plot of the

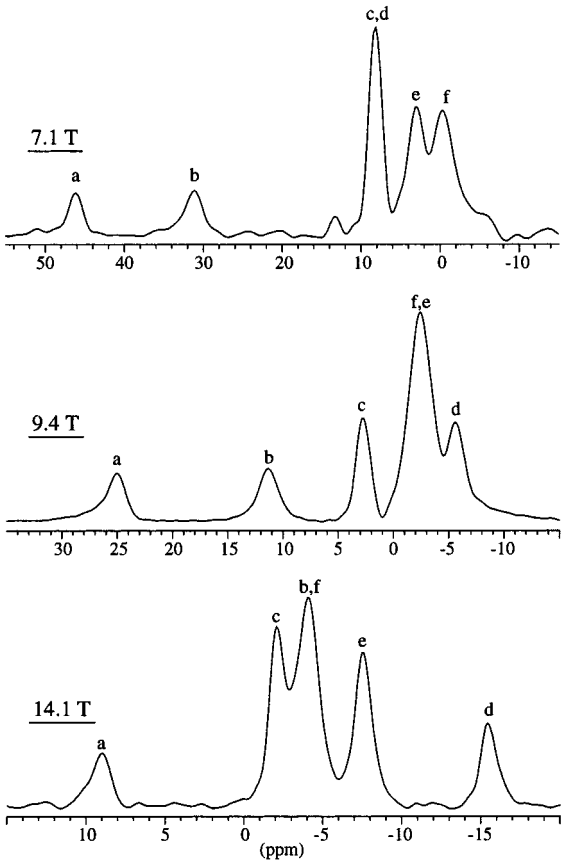

Figure 4. Isotropic projections from ^{23}Na MQMAS NMR spectra of $Na_6[P_2Mo_5O_{23}]\cdot 7H_2O$ recorded at 7.1, 9.4, and 14.1 T using spinning speeds of 13.0, 15.0, and 12.2 kHz, respectively. The spectra are obtained as summations over the resonances in the MQMAS spectra. The assignment of the six resonances is given by a−f, and the corresponding isotropic 3Q shifts (δ_{3Q}^{exp}) are summarized in Table 2.

Table 2. ^{23}Na Isotropic Triple-Quantum Shifts (δ_{3Q}^{exp}), Isotropic Chemical Shifts (δ_{iso}), and Quadrupolar Product Parameters (P_Q) for $Na_6[P_2Mo_5O_{23}]\cdot 7H_2O$ from ^{23}Na MQMAS NMR Spectra at 7.1, 9.4, and 14.1 T[a]

	δ_{3Q}^{exp} (ppm)				
	7.1 T	9.4 T	14.1 T	δ_{iso}[b] (ppm)	P_Q[b,c] (MHz)
Na(a)	45.8 ± 0.5	24.6 ± 0.5	8.8 ± 0.4	−1.6	3.15
Na(b)	30.9 ± 0.5	11.2 ± 0.5	−3.5 ± 0.3	−7.0	3.04
Na(c)	8.5 ± 0.4	2.4 ± 0.3	−2.3 ± 0.3	−2.7	1.69
Na(d)	7.5 ± 0.4	−5.9 ± 0.4	−15.6 ± 0.3	−11.0	2.49
Na(e)	2.6 ± 0.4	−3.1 ± 0.4	−7.7 ± 0.3	−5.2	1.66
Na(f)	−0.6 ± 0.4	−2.4 ± 0.4	−4.4 ± 0.3	−2.1	0.88

[a] The δ_{3Q}^{exp} and δ_{iso} values are relative to an external aqueous solution of 1.0 M NaCl. [b] Parameters determined from the dependency of δ_{3Q}^{exp} on the magnetic field strength (cf. eq 1 and Figure 5). [c] The quadrupolar product parameter is defined as $P_Q = C_Q(1 + \eta_Q^2/3)^{1/2}$.

δ_{3Q}^{exp} values as a function of $1/(32\nu_L^2)$ for the three different magnetic fields (Larmor frequencies, ν_L). Linear regression of these data employing eq 1 gives the δ_{iso} and P_Q values for the individual Na sites listed in Table 2.

A determination of the C_Q and η_Q parameters may be achieved from simulations of the individual line shapes observed in the F_2 dimension of the MQMAS spectra or from simulations of the line shapes for the central transitions observed in single-pulse ^{23}Na MAS experiments. Examination of the line shapes, obtained by summation over the individual resonances in the F_2 dimension of the MQMAS spectra, reveals that these are somewhat distorted especially at low magnetic field (7.1 T) and

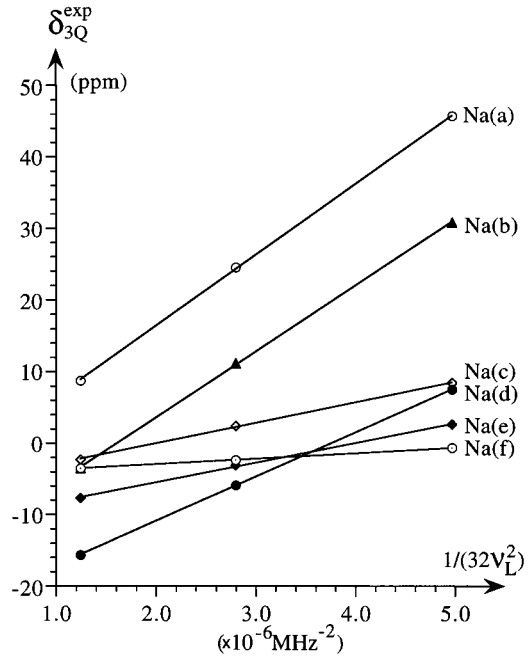

Figure 5. Plot of the isotropic 3Q shifts (δ_{3Q}^{exp}), observed at 7.1, 9.4, and 14.1 T for $Na_6[P_2Mo_5O_{23}]\cdot 7H_2O$, as a function of $1/(32\nu_L^2)$. The lines correspond to the results of linear regression analysis of the data, which gives the δ_{iso} and P_Q parameters for the ^{23}Na resonances listed in Table 2.

for the sites possessing strong quadrupolar interactions. This may reflect the fact that the excitation-conversion of 3Q coherences in MQMAS NMR depends strongly upon the magnitude of the quadrupolar coupling interaction and the applied rf field strength.[15,38,44] For most of the ^{23}Na sites, valuable estimates of C_Q and η_Q can be achieved from simulations of the F_2 summations employing fixed values for δ_{iso} (Table 2) and the restrictions on C_Q imposed by the P_Q parameters in Table 2. However, we find that an improved precision in the C_Q and η_Q parameters is obtained by least-squares fitting of six overlapping second-order quadrupolar line shapes to the central transitions observed in the single-pulse ^{23}Na MAS NMR spectra. As initial parameters in the optimizations we employ the estimated C_Q and η_Q values from the simulations of the F_2 summations and the δ_{iso} values in Table 2, obtained from the field dependence of the isotropic 3Q shifts.

The ^{23}Na MAS NMR spectrum of the central transition at 7.1 T is illustrated in Figure 6a and exhibits an improved resolution of the spectral features for the individual ^{23}Na sites as compared to the ^{23}Na MAS NMR spectra at 9.4 and 14.1 T. The optimized simulation of the six overlapping quadrupolar line shapes (with equal intensities) to the experimental central transition is shown in Figure 6b, while the traces shown below illustrate simulations of the individual line shapes for the six ^{23}Na resonances. The reliability of the C_Q and η_Q parameters, obtained from the 7.1 T spectrum, is confirmed by similar optimizations to the experimental ^{23}Na MAS NMR spectra recorded at 9.4 T (Figure 7a) and 14.1 T (Figure 7c). The optimized simulations corresponding to these spectra are shown in Figure 7b and Figure 7d, respectively, and are observed to convincingly reproduce all spectral features of the experimental line shapes for the central transitions.

(44) Amoureux, J.-P.; Fernandez, C.; Frydman, L. *Chem. Phys. Lett.* **1996**, *259*, 347.

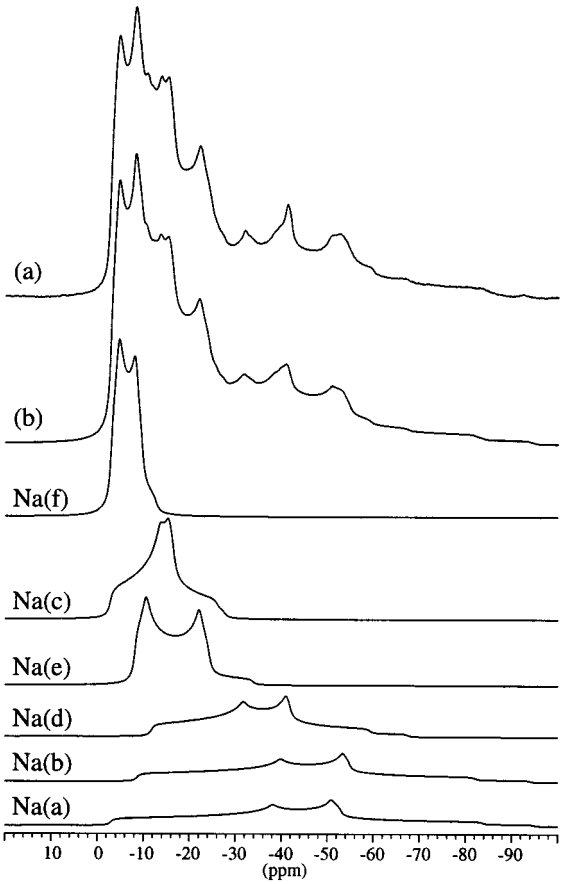

Figure 6. (a) ^{23}Na MAS NMR spectrum of the central transition for $Na_6[P_2Mo_5O_{23}]\cdot 7H_2O$ obtained at 7.1 T using a spinning speed of 7.0 kHz. (b) Optimized simulation of the central transition in spectrum a using six overlapping quadrupolar line shapes with equal intensities and corresponding to the C_Q, η_Q, and δ_{iso} parameters listed in Table 3 for Na(a)−Na(f). Simulations of the individual line shapes, which constitute the simulated spectrum in part b, are shown below the spectrum in part b and are indexed according to the parameters in Table 3.

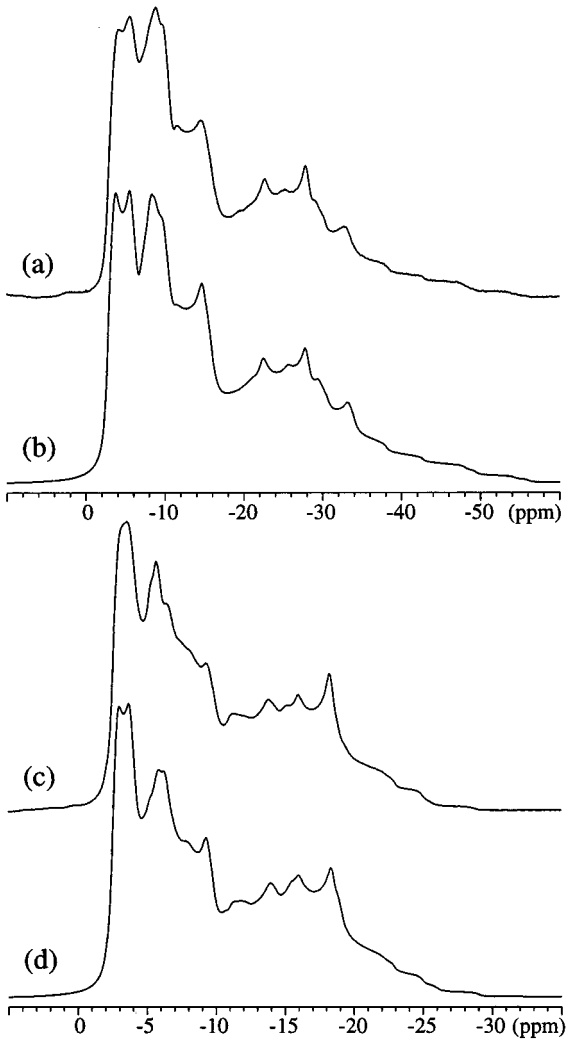

Figure 7. ^{23}Na MAS NMR spectra of the central transition for $Na_6[P_2Mo_5O_{23}]\cdot 7H_2O$ obtained at (a) 9.4 and (c) 14.1 T using spinning speeds of 11.0 and 11.8 kHz, respectively. Optimized simulations of the central transitions at (b) 9.4 and (d) 14.1 T corresponding to the C_Q, η_Q, and δ_{iso} parameters listed in Table 3.

The optimized C_Q, η_Q, and δ_{iso} parameters for the six sodium sites are listed in Table 3 along with error limits, which have been evaluated from the simulations of the experimental central transitions at the three magnetic fields. The isotropic chemical shifts in Table 2, as obtained from the field-dependence of δ_{3Q}^{exp}, are within the error limits of the δ_{iso} values given in Table 3. Furthermore, calculation of the P_Q parameters, using the C_Q and η_Q values in Table 3, gives P_Q values which on average deviate by only 0.05 MHz from those listed in Table 2. The excellent agreement between the data obtained from the ^{23}Na MQMAS and MAS NMR spectra is also apparent from a calculation of the isotropic 3Q shifts (δ_{3Q}^{calc}) using the C_Q, η_Q, and δ_{iso} parameters in Table 3. This gives mean deviations between δ_{3Q}^{calc} and δ_{3Q}^{exp} of 0.6, 0.4, and 0.3 ppm for the isotropic 3Q shifts at 7.1, 9.4, and 14.1 T, respectively, with the largest deviation being 1.2 ppm (Na(f) at 7.1 T).

The isotropic chemical shifts for $Na_6[P_2Mo_5O_{23}]\cdot 7H_2O$ fall in a range of 10 ppm, which partially accounts for the severe overlap of quadrupolar line shapes in the ^{23}Na MAS NMR spectra. A somewhat larger dispersion is observed for the quadrupolar couplings, which range from 1.02 to 2.94 MHz and fall into two groups corresponding to relatively small (Na(c), Na(e), Na(f)) and somewhat larger ((Na(a), Na(b), Na(d)) quadrupole couplings. Overall, the quadrupole couplings for $Na_6[P_2Mo_5O_{23}]\cdot 7H_2O$ are similar in magnitude to those reported for other sodium phosphates.[18,19] Finally, we note that the tetradecahydrate, $Na_6[P_2Mo_5O_{23}]\cdot 14H_2O$ (orthorhombic $P2_12_12_1$),[7] also contains six inequivalent sodium sites in the asymmetric unit. For this hydrate an assignment of the ^{23}Na quadrupole coupling parameters to the specific sodium sites in the reported crystal structure should be possible, which may improve the understanding between quadrupole coupling parameters and structural features for sodium salts of phosphomolybdate anions. Attempts are currently being made to obtain a pure sample of $Na_6[P_2Mo_5O_{23}]\cdot 14H_2O$ with the aim of characterizing this hydrate by ^{23}Na MAS and MQMAS NMR.

Table 3. ^{23}Na Quadrupole Coupling Parameters (C_Q and η_Q) and Isotropic Chemical Shifts (δ_{iso}) for $Na_6[P_2Mo_5O_{23}]\cdot 7H_2O$ from ^{23}Na MAS NMR Spectra at 7.1, 9.4, and 14.1 T[a]

	C_Q (MHz)	η_Q	δ_{iso}[b] (ppm)
Na(a)	2.94 ± 0.02	0.72 ± 0.02	−1.9 ± 0.3
Na(b)	2.85 ± 0.02	0.68 ± 0.02	−7.3 ± 0.3
Na(c)	1.50 ± 0.03	0.85 ± 0.03	−2.7 ± 0.2
Na(d)	2.31 ± 0.02	0.66 ± 0.02	−10.9 ± 0.3
Na(e)	1.70 ± 0.03	0.15 ± 0.03	−5.1 ± 0.2
Na(f)	1.02 ± 0.05	0.28 ± 0.03	−2.2 ± 0.2

[a] Assignment of the resonances according to the ^{23}Na MQMAS spectrum at 7.1 T, cf. Figure 4. [b] Isotropic chemical shifts relative to an external aqueous solution of 1.0 M NaCl.

Conclusions

The new hydrate of hexasodium diphosphopentamolybdate, $Na_6[P_2Mo_5O_{23}]\cdot 7H_2O$, has been characterized using a combination of ^1H, ^{23}Na, and ^{31}P MAS NMR spectroscopies and X-ray powder diffraction. The latter method has demonstrated that the hydrate is triclinic with the space group $P\bar{1}$. Quantitative ^1H MAS NMR has proven useful for the determination of the number of water molecules in the asymmetric unit, whereas ^{23}Na and ^{31}P MAS NMR have demonstrated that the asymmetric unit includes two different phosphorus sites and six nonequivalent sodium sites. The six sodium sites in $Na_6[P_2Mo_5O_{23}]\cdot 7H_2O$ have been clearly resolved in ^{23}Na MQMAS NMR spectra recorded at three magnetic fields, and ^{23}Na isotropic chemical shifts (δ_{iso}) and quadrupolar effect parameters ($P_Q = C_Q(1 + \eta_Q^2/3)^{1/2}$) have been determined from these spectra. Using these results, precise values for the quadrupole coupling parameters (C_Q and η_Q) and the isotropic chemical shifts have been obtained from simulations of the central transitions, observed in single-pulse ^{23}Na MAS NMR spectra at three magnetic fields. These data are in excellent agreement with the parameters δ_{iso}, P_Q, and δ_{3Q}^{exp} determined from the MQMAS NMR spectra, thereby illustrating the advantages of combining MQMAS and MAS NMR spectra at different magnetic fields for characterization of multiple sodium sites in inorganic systems.

Acknowledgment. The use of the facilities at the Instrument Centre for Solid-State NMR Spectroscopy, University of Aarhus, sponsored by the Danish Research Councils (SNF and STVF), Teknologistyrelsen, Carlsbergfondet, and Direktør Ib Henriksens Fond, is acknowledged. We thank the Aarhus University Research Foundation for equipments grants.

Supporting Information Available: List of observed and calculated X-ray diffraction peaks. This material is available free of charge via the Internet at http://pubs.acs.org.

IC000309J